Microchemical Journal 178 (2022) 107377

Contents lists available at ScienceDirect

Microchemical Journal

journal homepage: www.elsevier.com/locate/microc

Magnetic graphene molecularly imprinted polypyrrole polymer (MGO@MIPy) for electrochemical sensing of malondialdehyde in serum samples

Pablo Montoro-Leal [a], Mohammed Zougagh [b,c], Antonio Sánchez-Ruiz [d], Ángel Ríos [b,e], Elisa Vereda Alonso [a,*]

[a] Department of Analytical Chemistry, Faculty of Sciences, University of Málaga, Málaga, Spain
[b] Regional Institute for Applied Scientific Research, IRICA, Camilo José Cela Avenue, E-13005, Ciudad Real, Spain
[c] Department of Analytical Chemistry and Food Technology, Faculty of Pharmacy, University of Castilla-La Mancha, Albacete, Spain
[d] Department of Inorganic, Organic Chemistry and Biochemistry, Faculty of Pharmacy, University of Castilla-La Mancha, Albacete, Spain
[e] Department of Analytical Chemistry and Food Technology, Faculty of Science and Chemical Technologies, University of Castilla-La Mancha, Ciudad Real, Spain

ARTICLE INFO

Keywords:
Malondialdehyde
Derivatization
Molecularly imprinted polypyrrole
Magnetic graphene oxide
Serum samples

ABSTRACT

A modified screen-printed carbon electrode (SPCE) has been designed and fabricated for the determination of malondialdehyde (MDA), an important biomarker of oxidative stress. Magnetic graphene oxide (MGO) was synthesized and coated by a molecularly imprinted polypyrrole (MIPy) for the preparation of a novel hybrid nanomaterial (MGO@MIPy). The nanocomposite has been characterized using different spectroscopic and imaging techniques. The coupling of MIPy with MGO allows the exploitation of the magnetic properties of the material for separation, preconcentration and manipulation of analyte which is selectively captured onto the MIPy surface of the nanocomposite. Besides, the derivatization of MDA with diaminonaphtalene (DAN) was carried out, resulting in a more electroactive molecule (MDA-DAN). MDA-DAN was used as template in the synthesis of MIPy. SPCEs were employed to monitor the differential pulse voltammetry (DVP) levels of the material, which is related to the amount of the captured analyte. Under optimum conditions, the nanocomposite-based sensing system has proved to be suitable for the monitoring of MDA, presenting a wide linear range (0.01–100 μM), high sensitivity (experimental LOQ = 0.01 μM) and precision (RSD = 4%). For validation purposes, three chicken serum samples were analysed by external calibration, obtaining recoveries values close to 100% for all the spiked tests. Finally, the developed electrochemical sensor demonstrated to be adequate for bioanalytical application, presenting an excellent analytical performance for the routine monitoring of MDA in serum samples.

1. Introduction

Malondialdehyde (MDA) is a resultant product of lipid peroxidation, which has been widely used as biomarker for oxidative stress in medical diagnostic [1,2]. MDA can be found in biological samples such as plasma, serum, saliva, and urine [3–6], which arises from the oxidative degradation of polyunsaturated fatty acids [7]. MDA represents an important risk to the health of animals, including human beings, because of its reactivity with peptides, DNA, and nucleic acids [8,9]. It has been demonstrated that this molecule is involved in several serious human diseases such as diabetes, heart disorders, and cancer [9–11]. Therefore, the development of analytical methods for the determination of MDA in biological samples is essential. Different techniques have been applied in a variety of matrices for this purpose: chromatography [2,12–14], spectrofluorometry [15], and spectrophotometry [16]. However, the application of these analytical methods is often limited due to their high cost and involve time-consuming sample pre-treatment processes. Consequently, electrochemical sensors have become an important alternative, being easy for miniaturization and monitoring, low cost and high sensitivity [17,18] their most relevant advantages. These sensors incorporate recognition elements integrated with electrode that lead to an electrochemical signal upon analyte recognition. Due to the low electroactivity of MDA, there are few reports in the literature on its electrochemical determination [19–22]. These works

* Corresponding author.
E-mail address: eivereda@uma.es (E. Vereda Alonso).

https://doi.org/10.1016/j.microc.2022.107377
Received 10 January 2022; Received in revised form 7 March 2022; Accepted 8 March 2022
Available online 12 March 2022

used a glass carbon, Poly arginine-graphene quantum dots-chitosan, self-assembled riboflavin-taurine coupled with silver nanoparticles, multiwalled carbon nanotubes (MWCNTs) and gold surface modified by taurine film as transducing systems.

Molecular imprinting technology is a technique for the preparation of polymer-based adsorbents. In this approach, the functional monomer is polymerized in the presence of the target molecule (template) so that specific recognition sites are formed during the polymerization process. A large variety of methods for preparing molecularly imprinted polymers (MIP) can be found in the bibliography, and all of them rely on three basic steps: the formation of a complex by covalent or non-covalent bonding between the template molecule and the monomer; the polymerization process itself, and finally, the elution or elimination of the template from the polymer using electrochemical or chemical conditions to break the existing interactions between the template and the polymer. As a result, three-dimensional sites with similar size and shape as the target molecule are created. These specific sites are available for the recombination with the template molecule when this material is applied in the analysis of standard solutions and samples [23,24]. Molecularly imprinted polymers (MIPs) have been successfully applied for the determination of proteins, monosaccharides and drugs [25,26], and they have proven to be suitable as recognition elements in electrochemical sensors [27]. For electrochemical applications, the electrical properties of the elements involved in the MIP synthesis need to be adequate. For this reason, the use of conducting polymers or "synthetic metals" is critical. This kind of materials combines the properties of a polymer with the electric conductivity of a metal or a semiconductor, presenting a high number of conjugated double bonds in the structure. Among these polymers, polypyrrole (PPy) presents excellent advantages such as high electron-transfer capacity, simple preparation, low cost, stability, low toxicity and insolubility in water [27]. PPy can interact with organic and inorganic molecules via its extended aromatic structure and dipole moment. Some analytical methods based on conductive polymers for the preparation of MIPs have been previously reported, for example, for the determination of salicylic acid [27] and proteins [28] in biological samples, and organophosphates in environmental samples and agricultural products [29].

In recent years, the use of molecular imprinting technology has been extended to numerous research fields because of its advantages mentioned above [30,31]. Despite this, the electrochemical application of MIPs can be limited by long response times, poor electrocatalytic activity, and low sensitivity [32]. To compensate these disadvantages and improve electron-transfer capacity, some authors have reported the use of some well-known materials including graphene [33], carbon nanotubes (CNTs) [34], gold nanoparticles (Au NPs) [35], and graphene oxide (GO). GO is a monolayer material with an extended π-π system which has been widely used by researchers because of its adsorbent properties and ease of functionalization [36]. However, despite these improvements, other drawbacks in the preparation of MIP sensors, such as binding capacity, and problems to renew the spent MIP films have also been claimed. To solve these drawbacks, magnetic molecularly imprinted polymers have been shown to provide an effective way for immobilization and MIP renewal from the solid support. This kind of polymers bears selectivity due to its recognition element, and facilitate preconcentration, separation and manipulation of the analyte due to their magnetic properties. Several magnetic nanomaterials can be prepared with iron, nickel or cobalt for this use, being iron the most common substance due to their low-toxicity, biocompatibility, physiological stability and chemical properties, and high magnetic response [36,37].

In our case, the carrier was magnetic graphene oxide (MGO), which was fabricated by coupling of both $CoFe_2O_4$ nanoparticles and GO in a material that combine their excellent individual characteristics and properties [38]. A new nanocomposite material based on MGO and molecularly imprinted polypyrrole (MGO@MIPy) was designed to detect MDA specifically with extraordinary sensitivity and selectivity. MDA was derivatizated with diaminonaphtalene (DAN), resulting in a more electroactive molecule (MDA-DAN). In order to create the specific sites for MDA-DAN recognition, the correct interaction of the template with carrier and the monomer during the synthesis of the material is crucial. For this reason, MGO and PPy were also selected, presenting an aromatic domain compatible to interact with MDA-DAN throught π-π interactions during the synthesis of MGO@MIPy. HPLC, tandem mass spectrometry (MS-MS), UV–vis spectrophotometry, transmission electron microscopy (TEM), X-ray diffraction (XRD), and differential scanning calorimetry-thermogravimetric analysis (DSC-TGA) were applied to characterize the template and the proposed hybrid nanomaterial. The magnetic properties of MGO@MIPy were used for the easy and rapid modification of the SPCEs surface. On the other hand, differential pulse voltammetry (DVP) was the selected electrochemical technique to monitor the whole material on disposable SPCEs, which is related to the amount of the captured analyte on the surface of the material. The developed electrochemical sensor demonstrated to be adequate for bioanalytical applications, presenting an excellent analytical performance for the routine monitoring of MDA in serum samples. Finally, and to the best of our knowledge, no previous reports of a magnetic molecularly imprinted polypyrrole material for the electrochemical determination of MDA in biological samples was found, thus being this work a pioneering one in this area.

2. Experimental

2.1. Instrumentation

Electrochemical measurements were conducted by using a CHI842D electrochemical analyzer controlled by Chi842d software from CH Instruments (Austin, TX, USA). A three-electrode cell configuration was applied for the connection of the screen-printed carbon electrodes (SPCEs, DRP-110) from Dropsens (Oviedo, Spain) (a working carbon electrode of 4 mm diameter, a carbon counter electrode and a silver pseudo reference electrode). An interface DRP-BICAC70311 was used between the potentiostat unit and the screen-printed electrode.

The correct template preparation was verified by liquid chromatography/quadrupole-time-of-flight 6545 LC/Q-TOF from Agilent technologies (Santa Clara, CA, USA) and Secomam Uvi Light XS 2 spectrophotometer (Alés, France). The template was purified by using a combination of a modular LC Jasco system (Easton, MD, USA) consisting of an LC ternary pump (PU-2080 Plus), Sampler (AS-2055 Plus), column oven (CO-2065 Plus), a circular dichroism detector (JASCO CD-2095 PLUS), Agilent LC analytical column (model Sorbax Eclipse XDB-C18, 150 mm × 4.6 mm i.d., 5 μm particle size), and a Cole-Parmer microcomputer Controlled Fraction Collector CHF122SC with a 120 positions tray (Chicago, IL, USA). Data were acquired and the equipment controlled using CHROMNAV software, which was run under Microsoft Windows XP on an IBM compatible personal computer.

XRD patterns were measured on Philips model X'Pert MPD diffractomer using CuKα source (λ = 1.5418 A), programmable divergence slit, graphite monohromator and proportional sealed xenon gas detector. TGA and DCS graphs were obtained by Q50 and Q600 from TA instruments respectively. X-ray photoelectron spectroscopy (XPS) analysis were performed with a Physical Electronics ESCA 5701 instrument (Chanhassen, MN, USA); binding energies were observed, considering the position of the C 1 s peak at 284.8 eV. The residual pressure in the analysis chamber was maintained below 3×10^{-9} Torr during data acquisition. The microstructures of the new materials were observed and studied by transmission electron microscopy (TEM) JEOL, JEM-1400 (Peabody, MA, USA).

A Selecta ultrasound bath (Barcelona, Spain), a Hewlett Packard 5890, Series II gas chromatograph (WA, USA) and microcentrifuge Biosan Microspin 12 from LabNet Biotecnica S.L. (Madrid, Spain) were also used.

2.2. Solvents, reagents and samples

All aqueous solutions were prepared with analytical grade reagents and deionized water purified with a Milli-Q system from Millipore (Bedford, MA, USA) that reaches a resistivity of 18.2 MΩ·cm at 25 °C. Stock standard solution of Malondialdehyde bis(dimethyl acetal) was purchased from Sigma-Aldrich (St. Louis, MO, USA). For MGO and MGO@MIPy preparation, cobalt (II) chloride hexahydrate ($CoCl_2{\cdot}6H_2O$), iron (III) chloride hexahydrate ($FeCl_3{\cdot}6H_2O$), g-methacryloxypropyltrimethoxysilane (g-MPS), methacrylic acid (MAA), ethylene glycol dimethacrylate (EGDMA) and 2,2́-azobisisobutyronitrile (AIBN) were purchased from Sigma-Aldrich (St. Louis, MO, USA).

Graphite, sodium nitrate, potassium permanganate, hydrogen peroxide, sodium sulphite, tetraethyl orthosilicate (≥98%), 3-Aminopropyltriethoxysilane (≥99%), sulphuric acid (≥99%), hydrochloric acid (37%), methanol (≥99%), pyrrole (≥98%), 1,8-Diaminonaphtalene (≥98%) were obtained from Sigma-Aldrich (St. Louis, MO, USA). For template purification, ethanol (≥96%), acetonitrile (≥99%), formic acid (≥95%) and ammonium acetate (≥99%) were used as phase mobile and acquired from Merk (Darmstadt, Alemania). For sample preparation and electrochemical measurement, HCl was used as electrolyte and a lipid peroxidation (MDA) assay kit containing phosphotungstic acid solution (≥99%) and Butylated hydroxytoluene (BHT) (≥99%) was purchased from Merk (Darmstadt, Alemania). All solutions were stored in darkness at low temperature (-5°C) until use, except for the three chicken serum samples, which were stored in darkness at − 80 °C. Working solutions were daily prepared by derivatizing with DAN 5.8 mM solution prepared in HCl 2.4 M.

2.3. Synthesis of magnetic graphene oxide

$CoFe_2O_4$ nanoparticles were prepared in aqueous solution by following a previous reported method [39]. 10 mL water was used to dissolve 0.54 g $FeCl_3{\cdot}6H_2O$ and 0.238 g $CoCl_2{\cdot}6H_2O$, resulting in an aqueous solution. 1.2 g NaOH were dissolved in 10 mL water and added into the prepared solution under stirring at 80 °C. The stirring was continued for 30 min and cooled to room temperature and the precipitate was isolated in a magnetic field, and washed wish water three times. To modify the magnetic nanoparticles, tetraethyl orthosylicate (TEOS) (8 mL) was dissolved in ethanol (200 mL) and sonicated for 5 min. The pH of the solution was then adjusted to 4.5 using glacial acetic acid, and the solution was transferred to a round-bottom flask containing 1 g $CoFe_2O_4$ nanoparticles previously prepared. The resulting suspension was sonicated and stirred at 60 °C for 120 min. After this time, the suspension was decanted/filtered and the solid material was washed with deionized water two times followed by methanol, and vacuum-dried at room temperature. These silica-coated MNPs were dissolved/suspended in 150 mL of a 1% solution of 3-aminopropyltriethoxysilane (APTES) in 95% ethanol. The pH of this solution was adjusted to 4.5 with glacial acetic acid and stirred at 60 °C for 120 min. The obtained coated magnetic nanoparticles were then washed with deionized water three times, twice with methanol and vacuum-dried at room temperature.

GO was prepared according to a modified Hummers method [40]. The synthesis started by adding 0.5 g of graphite and 0.5 g of sodium sulphite, and the mixture was dispersed in 23 mL of concentrated sulphuric acid into 100 mL Erlenmeyer flask in an ice bath. It is important to remark that the temperature was maintained below 20 °C. This mixture was stirred for 4 h. After that, 3.0 g of potassium permanganate were added slowly to the reaction mixture and stirred the mixture for 1 h. After this hour, the ice was removed, and the reaction was stirred another hour more and heated at 35 °C. After this step, 46 mL of deionized water were added. The resulting reaction was stirred and heated at 95 °C for 2 h without allowing the mixture to boil. Subsequently, turn off the heater and allow it to cool in room temperature. Then, 100 mL of deionized water were added and stirred the mixture for 1 h. Now, 10 mL of 30 % hydrogen peroxide were added for 1 h with constant stirring. Finally, GO was formed, and the product was washed with deionized water several times until the pH became neutral, indicating the final product does not contain residual salts and acids.

500 mg of GO were suspended in ethanol (50 mL), and 500 mg of coated $CoFe_2O_3$ nanoparticles were added to this suspension. The mixture was sonicated for 10 min and the refluxed for 48 h. In this way, part of the MNPs were covalently attached to the GO sheet through an amide bond, which is formed by condensation between the acid groups of the GO surface and the amine groups of the MNPs. The resulting material was separated from the solution by using a permanent magnet.

Table 1
HPLC-Collector conditions.

Injection volume/μL	100
Column temperature/°C	50 ± 1
Mobile phase flow rate/mL·min^{-1}	1.0
Wavelenght/nm	311
Total run time/min	16.0
Window time/min	10.0–11.0
Column	Eclipse XDB-C18 4.6x150 mm
Mobile phase A	Acetonitrile 99%
Mobile phase B	Formic acid pH 2
Mobile phase C	30 mM ammonium acetate
Gradient program	10.0%A, 45%B, 45%C 8.0 min 100%A 3.0 min 10.0%A, 45%B, 45%C 5.0 min

2.4. Preparation of MDA-DAN solutions and purification of the template

A 5.8 mM solution of DAN in HCl 2.4 M was sonicated for 15 min and stored for one night at 4 °C. The resulting suspension was then centrifuged, and the supernatant was stored at 4 °C. This solution was found to be stable for at least one week at 4 °C. A separate 1 M solution of malondialdehyde bis(dimethyl acetal) was prepared by diluting the commercial 6.1 M solution in methanol. Standards in the 0.01–100 μM range were prepared daily by dilution of a 1 mM stock solution of MDA, and derivatized with DAN under acidic conditions through a previously reported procedure to give the corresponding naphtodiazepinium chloride [41]. Briefly, malondialdehyde bis(dimethyl acetal) standard solutions were hydrolyzed in situ to form MDA under acidic conditions. Then, 900 μL of DAN solution prepared in HCl were added to the MDA solution. The final volume was then adjusted to 1 mL with deionized water and the reaction mixture was kept at 37 °C for 180 min. The formation of DAN/MDA was confirmed through MS/MS and UV–Vis analysis.

In order to avoid interferences in the MGO@MIPy synthesis, an additional separation process was conducted when MDA-DAN solution was used as template; thus, 125 μL of malondialdehyde bis(dimethyl acetal) 1 M solution was derivatized with 25 mL of 5.8 mM DAN in 2.4 M HCl under the previously described conditions to afford a 5 mM MDA-DAN solution. The MIPs synthesized with low-purity templates often suffer from several drawbacks such as lack of selectivity and sensitivity. The impurities or interferences with similar structures compete with the template in the formation of imprinting complex before polymerization, therefore reducing the recognition ability toward the target molecule and disturbing the interaction of the target template and the functional monomer [42]. For this reason, the resulting MDA-DAN solution was then partitioned into 500 uL portions and purified through HPLC using a fraction collector. 100 injections of 100 μL (5 per chromatographic vial) were conducted, yielding 100 mL of pure MDA-DAN acetonitrile solution. The HPLC and collector conditions are summarized in Table 1. Three different solutions were involved in the chromatographic gradient (acetonitrile 99%, ammonium acetate 30 mM and formic acid solution at pH 2), which were previously used for MDA-DAN HPLC analysis [41]. Wash solution was ethanol/water (80/20 v/v). Finally, a N_2 current and a water bath at 80 °C was used to preconcentrate by acetonitrile evaporation from 100 mL to 3 mL (final concentration 17 mM). The

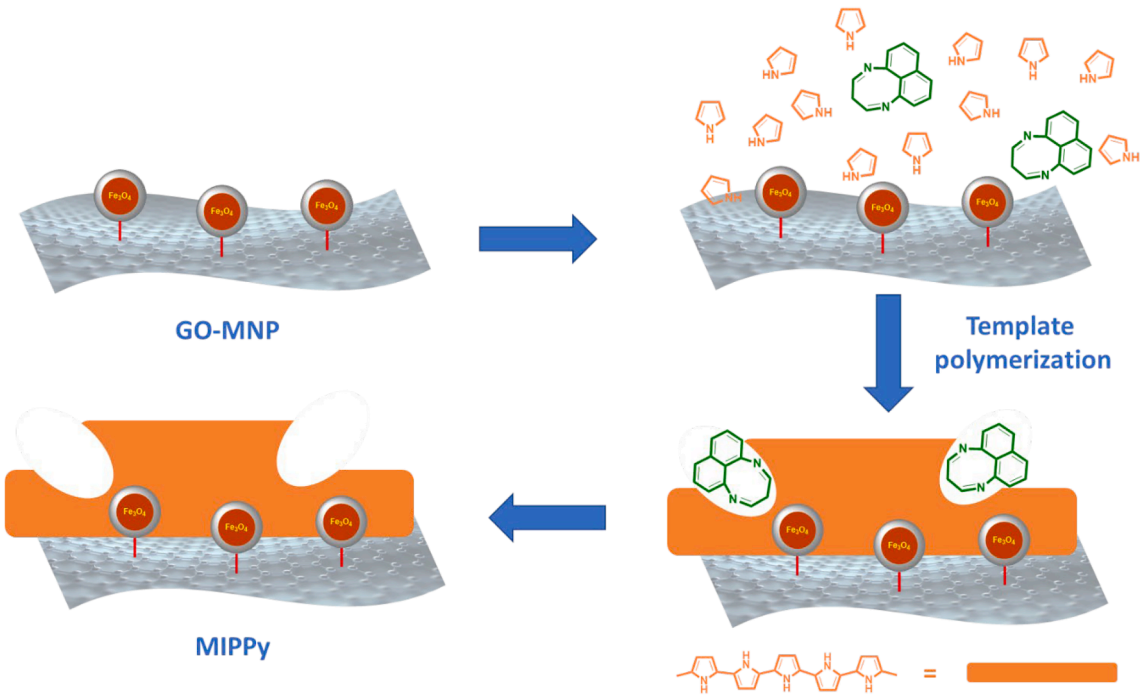

Fig. 1. Synthesis of MGO@MIPy.

preconcentrated final solution was analyzed by means of UV–Vis spectroscopy for confirmation.

2.5. MGO@MIPy synthesis

MGO@MIPy synthesis was conducted according to a previously reported procedure [27]: 1.5 mL of purified MDA-DAN solution (equivalent to 5 mg of MDA-DAN) was added to a solution of 25 μL of pyrrole monomer in 0.5 mL of acetonitrile. In parallel, 30 mg of MGO was suspended in 10 mL of HCl 10% solution and sonicated for 20 min. This suspension was then added to the previous pyrrole solution, maintaining stirring for 10 min. Separately, 120 mg of $FeCl_3$ was dissolved in 1 mL HCl 10% and added dropwise. After 10 min of stirring, the obtained material was washed four times with ethanol: acetic acid (1:1, v/v) while using an external magnetic field, and then dried at 80 °C. The magnetic molecularly non-imprinted polypyrrole (MGO@NIPy) was prepared analogously to MGO@MIPy, but without the MDA-DAN template. The resulting material was characterized with XRD, FTIR, TEM and TGA. The synthesis process can be observed in Fig. 1.

2.6. Sample preparation

20 μL of serum sample were gently mixed with 500 μL of 42 mM sulfuric acid in a microcentrifuge tube. 125 μL of phosphotungstic acid solution was added and mixed by vortexing. The suspension was incubated at room temperature for 5 min and then centrifuged at 13,000 rpm for 3 min. In a separate tube, 2 μL of BHT was added to 100 μL of water. The resulting pellet was resuspended on ice with the water/BHT solution. Finally, to form the MDA-DAN adduct, DAN in 2.4 M HCl solution was added into the vial containing sample to adjust the final volume from 100 μL to 1 mL. The solution was incubated at 37 °C for 180 min.

2.7. Sensor modification and measurement

A 0.5 $g{\cdot}L^{-1}$ suspension of MGO@MIPy was prepared in ethanol and sonicated for 20 min. Separately, a Nd/Fe/B magnet was fixed on the back of the screen-printed carbon electrodes by using a double face adhesive tape. Then, 2.5 μL of the suspension previously prepared was deposited to cover the working electrode surface. As a result, the material was retained by the external magnetic field and the working electrode surface was modified. Finally, ethanol was evaporated using heated air. After the surface modification, the screen-printed electrode was connected to the electrochemical analyser. Then, a 50 μL drop of standard or sample was deposited onto the electrode. Differential pulse voltammetry (DPV) was the electrochemical technique used for MDA-DAN determination, and the experimental conditions were the following: initial E of 0.7 V, final E of 1.0 V, 0.05 V amplitude, pulse width 0.05 s, pulse period 0.5 s and quiet time 2 s. The electrochemical experiments were performed at room temperature.

3. Results and discussion

3.1. Template characterization results

8 μL of a non-purified solution containing derivatized MDA was injected in LC/Q-TOF to obtain the MS/MS spectrum. The peaks 158.0844 and 194.0844 were found, corresponding to the compound $C_{10}H_{10}N_2$ (DAN excess) and $C_{13}H_{10}N_2$ (MDA-DAN) with > 95% score. The reported chromatographic method separated adequately MDA-DAN from the excess of DAN, and the distance between retention times and its repeatability allows the purification by HPLC-collector coupling. The chromatogram can be observed in supplementary material (Fig. S1). UV–vis spectra of MDA-DAN solution were obtained before and after purification process and compared with DAN solution spectrum (in 280–350 nm range). According to bibliography, MDA-DAN presents a characteristic spectrum with two peaks at 311 and 326 nm[41], while DAN spectrum is quite different, appearing an absorption band at 280 nm. As can be observed in Fig. S2, there was a middle situation in non-purified MDA-DAN solution spectrum, presenting characteristic bands of both DAN and MDA-DAN adduct. In purified MDA-DAN spectrum, there was no absorption band associated with DAN. Therefore, the purification process was succeeded, eliminating DAN excess from the solution.

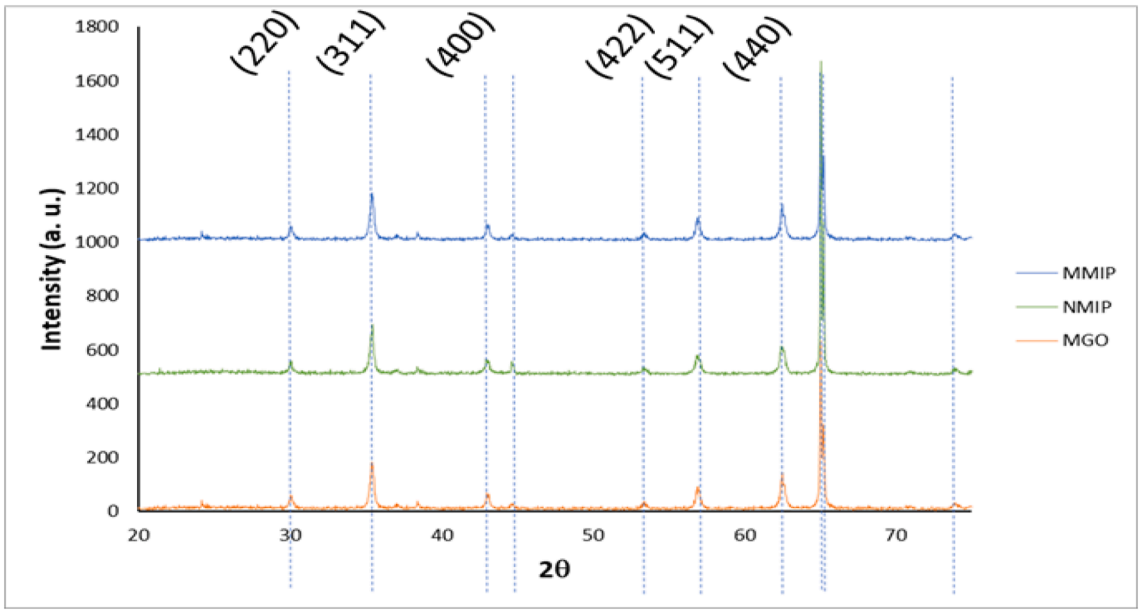

Fig. 2. XRD spectra MGO, MGO-NMIP and MGO-MMIP. Refraction planes are depicted above each peak.

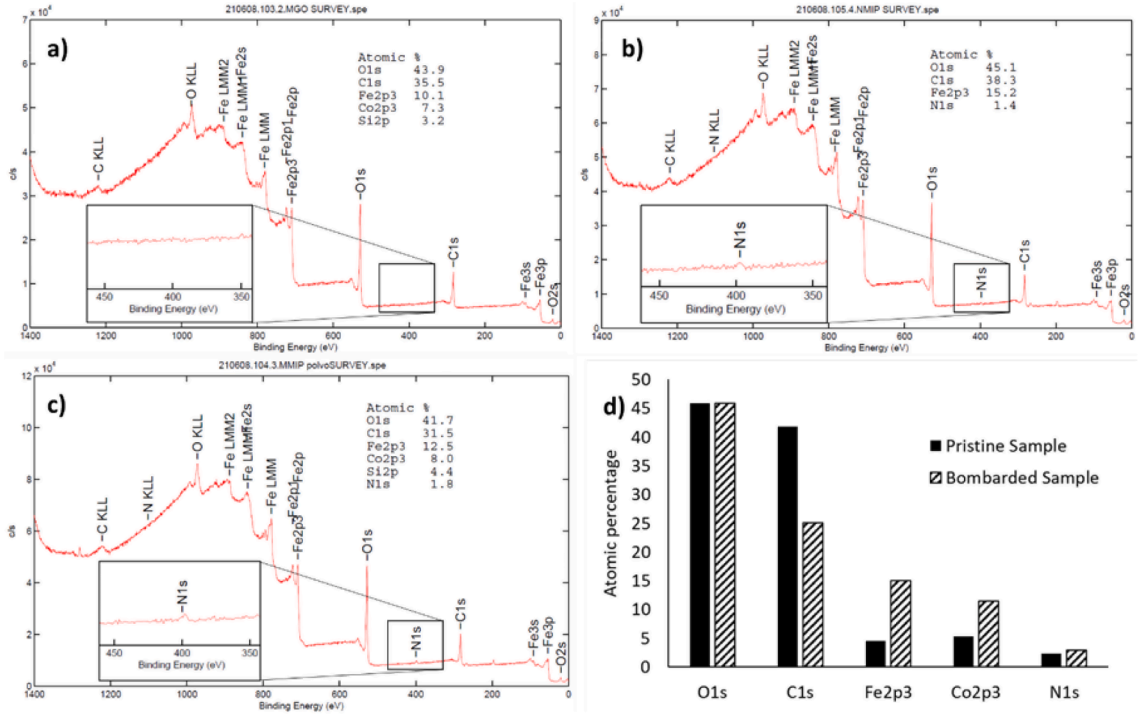

Fig. 3. XPS profiles of a) unmodified magnetic graphene oxide (MGO), b) magnetic graphene oxide modified with non molecularly imprinted polypyrrole (MGO-NMIP) and c) magnetic graphene oxide modified with molecularly imprinted polypyrrole (MGO-MMIP). d) Depth profile of MGO-MMIP sample before (black bars) and after (striped bars) bombardment with Ar + ions for 0.5 min.

3.2. MGO and MGO@MIPy characterization results

All prepared materials were analyzed through different techniques. XRD indicated that the magnetic nanoparticles remained stable throughout the whole polymerization process, as can be seen from the diffractions showed in Fig. 2, at 30.2°, 35.5°, 43.1°, 45.0°, 53.5°, 57.1° and 62.4° are observed, all corresponding to cobalt-iron oxide nanoparticles.

The atomic composition was studied through XPS. Graphene-supported magnetic nanoparticles showed the expected peaks for C, Fe and Co (not shown in the picture for clarity); modification with polypyrrole, either molecularly imprinted or not, originated the appearance of N1s peak, corresponding to the polymer. As can be observed in Fig. 3, the depth profile of the material revealed that upon argon bombardment, the percentage of carbon decreased from 42% to 26%, while iron and cobalt increased from 4.5% and 5.4% to 15% and 11.5%, respectively. Nitrogen concentration remained unaltered, suggesting that the polymer layer surrounded the magnetic nanoparticles, thus yielding a constant percentage of this element.

TEM images showed that MGO consists of an agglomerate of Fe-Co

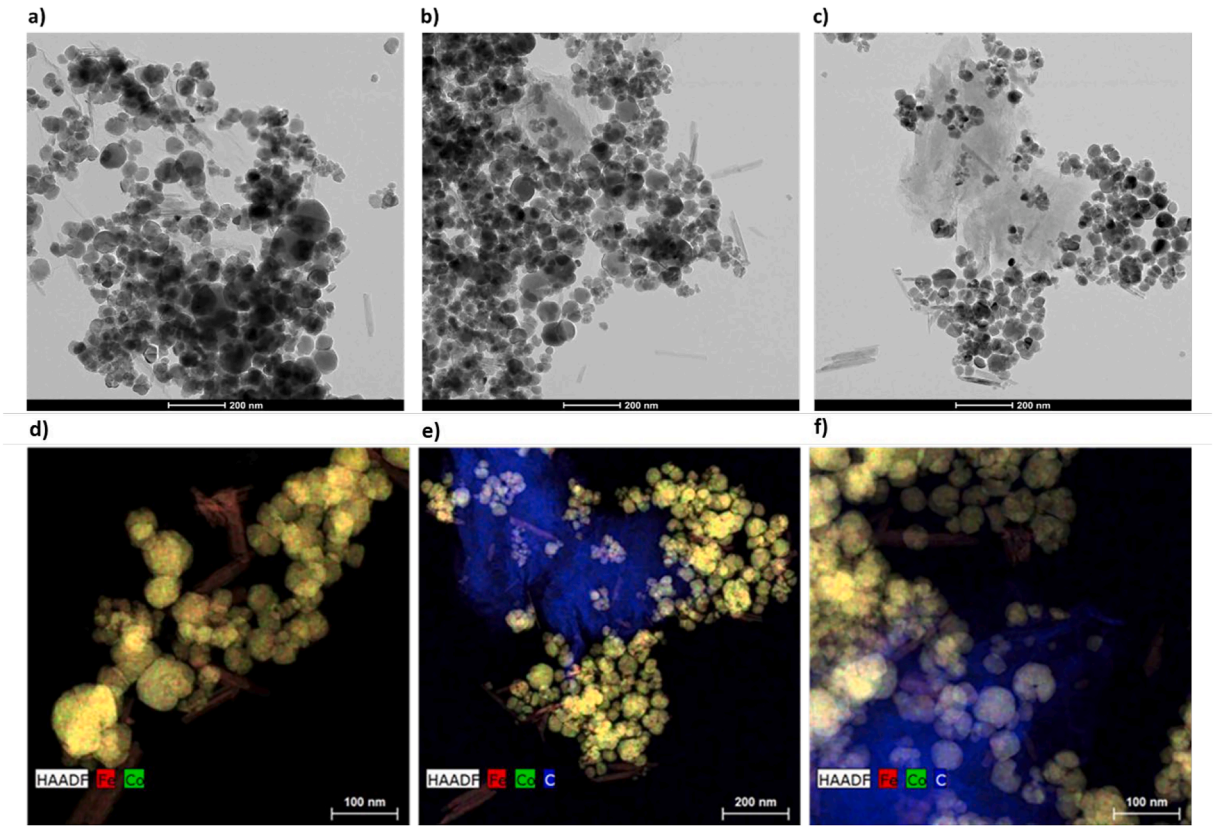

Fig. 4. TEM images of a) unmodified MGO, 200 nm b) MGO-NMIP 200 nm and c) MGO-MMIP 200 nm. HAADF -TEM images of d) unmodified MGO, 100 nm e) MGO-NMIP, 200 nm and f) MGO-MMIP, 100 nm.

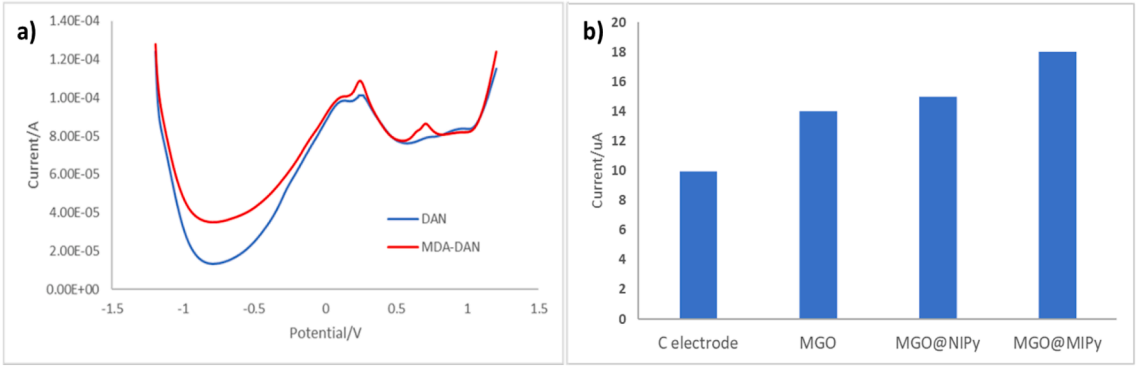

Fig. 5. a) Differential pulse voltammograms of DAN and non-purified MDA-DAN solutions using MGO@MIPy as surface modifier and b) Peak height obtained when a MDA-DAN 0.1 mM solution was measured, comparing the signal of regular carbon electrodes and the signal obtained using MGO, MGO@NIPy and MGO@MIPy as surface modifiers.

nanoparticles with graphene sheets intercalated among them (Fig. 4a, 4b and 4c). Upon formation of the polypyrrole polymer, an additional layer of material can be seen, especially in Fig. 4c, which embeds both the nanoparticles and the graphene fragments. This arrangement can be seen more clearly in the high-angle annular dark field, HAADF-TEM images (Fig. 4d, 4e and 4f), in which the nanoparticles are depicted in yellow, as they are composed of iron (red) and cobalt (green). The bare nanomaterial forms spherical nanoparticles with graphene sheets between them (Fig. 4a). In the polypyrrole material, both in the non-molecularly imprinted (4b) or imprinted (4c), the polymer acts as a matrix that embeds the nanoparticles and the graphene sheets, forming a conductive hybrid material that could explain the electrochemical behaviour of the electrode and its high sensitivity towards the analyte.

DSC-TGA analysis showed two evaporation peaks at temperatures depicted in Fig. S3. The first peak was assigned to sample moisture, and the second one, to the evaporation of APTES from the coating of the magnetic nanoparticles. MGO sample showed a steep weight loss at 750 °C, which was assigned to the decomposition of the graphene sheets. In the polypyrrole-coated samples, however, the expected maximum weight loss at around 350–450 °C for the polymer was not present. Instead, a progressive weight loss was observed during all the temperature range, with a steep loss from 700 °C onwards. This behaviour was attributed to a more controlled heat absorption through the graphene sheets and the nanoparticles that prevented a sudden weight loss as in the case of polypyrrole alone.

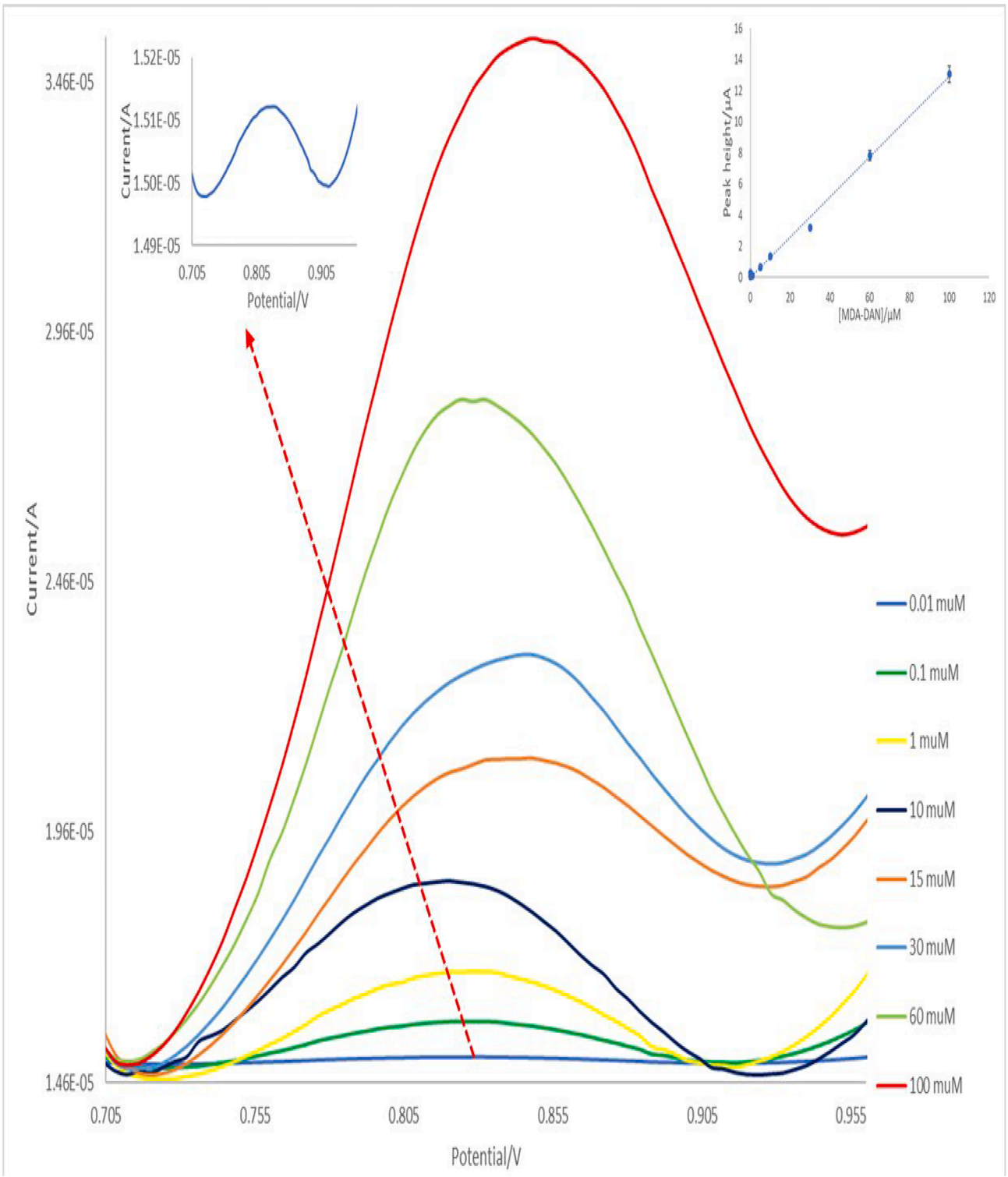

Fig. 6. DPV responses of calibration standards.

3.3. Electrochemical behaviour

MDA was determined by using DPV technique. In order to assign correctly the electrochemical peak of MDA-DAN, a non-purified MDA-DAN 0.1 mM solution voltammogram was compared with, and a blank solution containing DAN (Fig. 5a). In both experiments, the current profile was studied from −1.4 V to 1.4 V, HCl 2.4 M was used as electrolyte and the working electrode surface was modified with MGO@-MIPy. As can be seen in Fig. 5a, blank and non-purified MDA-DAN solutions presented an oxidation peak between 0 and 0.5 V. According to the investigation developed by G. Wang, this electrochemical behaviour can be observed in DAN molecules and derivatives [43]. Therefore, this peak can be assigned to DAN due to the presence of this molecule in both solutions. Besides, an additional oxidation peak at 0.85 V in MDA-DAN spectrum can be observed. Therefore, the potential range 0.7–1.0 V was selected for the determination of MDA-DAN. The current profile of regular carbon electrode and modified carbon electrodes using GO and MGO as modifiers were performed in 0–1.0 V range (Fig. S4). No

electrochemical peak can be seen in the voltammograms corresponding to GO and MGO, demonstrating that there is no signal contribution of those materials to the current profiles of DAN (blank solution) and non-purified MDA-DAN voltammograms in the studied range. In addition, the signal behaviour when the electrode surface was modified with different materials is shown in Fig. 5b. For this purpose, MDA-DAN 0.1 mM solution was measured using HCl 2.4 M as electrolyte, comparing with the signals obtained when MGO, MGO@NIPy and MGO@MIPy were used as modifiers. The signal with MGO was greater than the signal obtained with the regular carbon electrode, from 10 to 14 μA (a signal increasing of 40%). The oxidation peak was even greater and pronounced when the electrode surface was modified with MGO@NIPy (15 μA) and MGO@MIPy (18 μA), a signal increasing of 50% and 80%, respectively (referenced to the oxidation peak obtained with the regular carbon electrode). The presence of PPy in the material increased the electrochemical signal, and MGO@MIPy presented the highest peak. It can be concluded that the sensibility of the sensor was improved when the magnetic imprinted material was used as modifier.

3.4. Optimization results

The following parameters were optimized by using a univariant strategy, changing one parameter and keeping the other constant: The proportion magnetic carrier/template (w/w) during MGO@MIPy synthesis, electrolyte concentration, drop volume and amount of surface modifier. For optimization purpose, a 0.1 mM MDA-DAN solution was measured to perform the experiments, using peak height as the analytical response and HCl 2.4 M as electrolyte (except for the optimization electrolyte concentration). The experimental conditions for electrochemical measurement were the same mentioned above in experimental section.

For the optimization of the proportion magnetic carrier/template (w/w), 30 mg of MGO remained constant and the synthesis was performed separately with 0, 0.5, 1, 2, 5 and 10 mg of template. The resulting material with 0 mg of template is also called MGO@NIPy. Then, the MDA-DAN solution was measured by using the different synthesized materials, and the results are shown in Fig. S5a. As can be observed, the electrochemical signal increased from 0 to 5 mg, remaining constant from 5 to 10 mg. This behaviour demonstrated that the specific sites for the recognition of the analyte were adequately generated, increasing the number of available sites, and reaching the maximum when 5 mg or superior amount of template was used. Therefore, 5 mg was selected as the optimum amount of MDA-DAN to perform the synthesis.

The electrolyte concentration was also optimized. For this purpose, MGO@MIPy was used as modifier and the measuring conditions were maintained except for the HCl concentration, studied in the 0.1–3.0 M range. The results can be observed in Fig. S5b, the electrochemical signal increased from 0.1 to 1.2 M and remained constant from 1.2 to 3 M. Consequently, 900 μL of DAN solution in 2.4 M HCl was used to prepare standard and samples with a final volume of 1 mL (resulting in 2.2 M HCl), forming the MDA-DAN adduct and adjusting the electrolyte concentration into the optimum range simultaneously.

The amount of surface modifier and drop volume were also studied in the 25–50 μL and 1.25–15 μg ranges, respectively. However, a non-significant change during the optimization process was observed. Therefore, the minimum amount of material to modify adequately the working electrode surface was selected, corresponding to 1.25 μg (2.5 μL of 0.5 $g{\cdot}L^{-1}$ MGO@MIPy suspension). Besides, 50 μL of drop volume was selected in order to cover easily the three electrodes during the measurement.

3.5. Figures of merits and application

After optimization, analytical features of the reported sensor were determined. The calibration curve was prepared in the range of 0.01 μM – 100 μM (Fig. 6) and the signal was studied by using the peak height (μA), presenting the following linear calibration: $I_p = 0.1867 \cdot C_{MDA\text{-}DAN} - 0.2893$ ($r^2 = 0.998$). For reproducibility evaluation, four electrodes (n = 10) were used to measure a standard MDA-DAN solution 50 μM and calculate the relative standard deviation (RSD), providing a 4%. LOQ of the method was not calculated with the classical signal-to-noise ratio. Alternatively, other criteria can be used by authors, defining the low limit of quantification (L-LOQ) as the minimum level of MDA-DAN which presents good linear relationship [19]. Therefore, the standard corresponding with the minimum MDA-DAN concentration of the linear calibration was selected as the L-LOQ of the method (0.01 μM). According to IUPAC definition, LOD = (3/10) · LOQ. Therefore, LOD of the method can be estimated as 0.003 μM. These results evidenced the good sensitivity and precision of the proposed MDA sensor.

Table 2
Analysis performed for the determination of MDA in chicken serum samples.

Sample	Added/μM	Found/μM	Recovery/%	$t_{calculated}$ [a]
Serum 1	–	–	–	–
	12	13.1 ± 0.6	109	3.2
	18	17.4 ± 0.6	97	1.7
	24	23 ± 2	96	0.9
Serum 2	–	–	–	–
	12	14 ± 1	120	3.5
	18	16.9 ± 0.6	94	3.2
	24	21 ± 2	89	2.6
Serum 3	–	–	–	–
	12	12 ± 2	100	0.0
	18	18 ± 1	100	0.0
	24	21 ± 1	89	4.2

[a] *t*-test to compare one sample mean and an accepted value.

For validation purpose, the analysis of three real chicken serum samples were performed in triplicate under optimum conditions, and the accuracy was studied by using spike tests in the real samples. From the results shown in Table 2, it can be observed that all recoveries were close to 100% for all the spiked samples. Two statistical tests were applied for a 95% confidence level and no significant differences were observed comparing the concentration values obtained by the proposed method and the spike: Paired sample *t*-test, $t_{calculated} = 1.12 < t_{tabulated} = 2.31$, assuming constant variance, and *t*-test to compare one sample mean and an accepted value (the concentration added), $t_{calculated}$ from Table 2 < $t_{tabulated} = 4.3$. Furthermore, the samples were analysed by external calibration, so it can be confirmed that this method does not present any interference from these complex matrices.

In Table 3 a comparative study of previous alternative methods reported in bibliography for the determination of MDA can be observed, including electrochemical [1,19–22], fluorometric [44], and chromatographic methods [13,45,46]. In general, the estimated L-LOQ and RSD values were significantly lower or in the same order than other reported methods, except for the LOQ reported by Hasanzadeh et al [20]. Nevertheless, as has been said above, the proposed method was considered to be free of interferences, while the rest of compared methods used standard additions calibration to avoid matrix effects or calibration method was not reported, except for the analytical method reported by Bertolín et al [13]. Moreover, this method used one of the most extended linear ranges, presenting one of the best analytical features.

4. Conclusions

A novel modified screen-printed electrode has been designed and fabricated for the determination of MDA by using MGO@MIPy as surface modifier. The use of MGO as magnetic carrier allowed the exploitation of its magnetic properties, retaining the material over the working electrode surface by using an external magnetic field. As a result, the modification process is rapid and effective. Moreover, the presence of PPy in the material resulted in a remarkable amplification of the signal.

Table 3
Comparative study of electrochemical methods for MDA determination.

Instrument/ Electrode	Modification	LOQ/μM	Precision/%	External calibration	Linear range/μM	Ref
GCE[a]	PARG-GQDs-CS[b]	0.006	2.1	No	0.006–100	[19]
GCE	PARG-GQDs	0.0003	6.0	No	0.06–0.2	[20]
GCE	RF-PT-AgNPs[c]	590	No reported	No	620–890	[1]
Au	PT[d]	0.02	15	No	0.02–3	[21]
GCE	MWCNTs	0.1	Not reported	No	0.1–90	[22]
FS[e]	–	0.1	Not reported	No	0.1–20	[44]
HPLC-UV	–	0.07	4.64	No	0.07–42	[45]
GC-FID[f]	–	0.07	5.3	No	0.07–56	[46]
UPLC-FLD[g]	–	0.1	7.3	Yes	0.02–40	[13]
UPLC-DAD[h]	–	0.4	9.5	Yes	0.25–40	[13]
SPCE	MGO@MIPy	0.01	4.0	Yes	0.01–100	This work

[a] Glass-carbon electrode.
[b] Poly arginine-graphene quantum dots-chitosan.
[c] Self-assembled riboflavin-taurine coupled with silver nanoparticles.
[d] Polytaurine.
[e] Fluorescence spectrometer.
[f] Gass chromatography with flame ionization detector.
[g] Ultraperformance liquid chromatography with a fluorescence detector.
[h] Ultraperformance liquid chromatography with diode array detector.

On the other hand, the derivatization of MDA with diaminonaphtalene (DAN) was carried out, resulting in an aromatic electroactive molecule (MDA-DAN). This sensor has proven to not be susceptible to suffer interferences thanks to specific recognition sites generated. In addition, the preparation of the template and the magnetic nanomaterials MGO and MGO@MIPy was succeeded and confirmed by several characterization techniques. Besides, some synthesis and measurement parameters were adequately optimized by following an univariant strategy. In this work, the analytical performance was studied under optimum conditions and compared with electrochemical and alternative analytical methods previously reported in bibliography, presenting good sensitivity, suitable precision, and excellent selectivity. For validation purpose, three serum samples were analysed by external calibration, obtaining high recoveries values. Therefore, the developed electrochemical sensor has demonstrated its applicability in the biomedicine field, presenting an excellent analytical performance for the routine monitoring of MDA in serum samples. Finally, and to the best of our knowledge, there is no previous report of a magnetic molecularly imprinted polypyrrole material for the electrochemical determination of MDA in biological samples.

CRediT authorship contribution statement

Pablo Montoro-Leal: Investigation, Validation, Writing – original draft. **Mohammed Zougagh:** Conceptualization, Resources, Methodology, Writing – review & editing. **Antonio Sánchez-Ruiz:** Conceptualization, Writing – original draft, Writing – review & editing. **Ángel Ríos:** Supervision, Project administration, Funding acquisition. **Elisa Vereda Alonso:** Methodology, Writing – review & editing.

Declaration of Competing Interest

The authors declare that they have no known competing financial interests or personal relationships that could have appeared to influence the work reported in this paper.

Acknowledgements

The Spanish Ministry of Science and Innovation, JJCC Castilla-La Mancha and Junta de Andalucía are gratefully acknowledged for funding this work with Fellowship FPU18/05371, and Grants PID2019-104381 GB-I00, JCCM SBPLY/17/180501/000262, and UMA18FEDERJA060, respectively. Funding for open access charge: Universidad de Málaga /CBUA.

Appendix A. Supplementary data

Supplementary data to this article can be found online at https://doi.org/10.1016/j.microc.2022.107377.

References

[1] M. Jafari, E. Solhi, S. Tagi, M. Hasanzadeh, V. Jouyban-Gharamaleki, A. Jouyban, N. Shadjou, Non-invasive quantification of malondialdehyde biomarker in human exhaled breath condensate using self-assembled organic-inorganic nanohybrid: A new platform for early diagnosis of lung disease, J. Pharm. Biomed. Anal. 164 (2019) 249–257.
[2] X. Dong, J. Tang, X. Chen, Sensitive determination of malondialdehyde in rat prostate by high performance liquid chromatography with fluorescence detection, Sci. Rep. 10 (2020) 3990.
[3] J.-A. Oh, H.-S. Shin, Simple and sensitive determination of malondialdehyde in human urine and saliva using UHPLC–MS/MS after derivatization with 3,4-diaminobenzophenone, J. Sep. Sci. 40 (20) (2017) 3958–3968.
[4] R.S. Kushwaha, R.C. Gupta, S. Sharma, T. Masood, J.P. Sharma, R.K. Singh, R. K. Singh, C.L. Gierke, G. Cornelissen, Chronomics of Circulating Plasma Lipid Peroxides and Antioxidant Enzymes in Renal Stone Formers, Indian J. Clin. Biochem. 34 (2) (2019) 195–200.
[5] J. Aguilar Diaz De Leon, C.R. Borges, Evaluation of oxidative stress in biological samples using the thiobarbituric acid reactive substances assay, Journal of Visualized Experiments. 2020 (2020) 61122.
[6] S. Ersan, B. Cigdem, D. Bakir, H.O. Dogan, Determination of levels of oxidative stress and nitrosative stress in patients with epilepsy, Epilepsy Res. 164 (2020), 106352.
[7] S. Khezrian, A.P. Salati, N. Agh, H. Pasha-Zanoosi, Effect of replacement of fish oil with different plant oils in oncorhynchus mykiss broodstocks diets on egg and larval antioxidant defense development, Veterinary Research, Forum. 11 (2020) 83–88.
[8] J. ben Salah-Abbès, H. Belgacem, K. Ezzdini, M.A. Abdel-Wahhab, S. Abbès, Zearalenone nephrotoxicity: DNA fragmentation, apoptotic gene expression and oxidative stress protected by Lactobacillus plantarum MON03, Toxicon. 175 (2020) 28–35.
[9] J. Zińczuk, M. Maciejczyk, K. Zaręba, A. Pryczynicz, V. Dymicka-Piekarska, J. Kamińska, O. Koper-Lenkiewicz, J. Matowicka-Karna, B. Kędra, A. Zalewska, K. Guzińska-Ustymowicz, Pro-oxidant enzymes, redox balance and oxidative damage to proteins, lipids and DNA in colorectal cancer tissue. Is oxidative stress dependent on tumour budding and inflammatory infiltration? Cancers. 12 (2020) 1–20.
[10] E. Romuk, C. Wojciechowska, W. Jacheć, J. Nowak, J. Niedziela, J. Malinowska-Borowska, A. Głogowska-Gruszka, E. Birkner, P. Rozentryt, Comparison of Oxidative Stress Parameters in Heart Failure Patients Depending on Ischaemic or Nonischaemic Aetiology, Oxid. Med. Cell. Longevity 2019 (2019) 7156038.
[11] M. Madi, S.G. Babu, S. Kumari, S.R. Shetty, S. Bhat, R. Castelino, Lipid peroxidation marker in saliva of type 2 diabetes mellitus with oral manifestations – A clinical and biochemical study, Bangladesh Journal of, Medical Science. 17 (2018) 644–651.
[12] M. Mirmoghaddam, M. Kaykhaii, M. Hashemi, A.J. Keikha, S.H. Hashemi, H. Yahyavi, Application of response surface modeling for optimization and

determination of malondialdialdehyde by vortex-assisted dispersive liquid-liquid microextraction and GC-FID, J. Chil. Chem. Soc. 64 (2019) 4531–4537.
[13] J.R. Bertolín, M. Joy, M. Blanco, Malondialdehyde determination in raw and processed meat products by UPLC-DAD and UPLC-FLD, Food Chem. 298 (2019), 125009.
[14] N. Vanova, L. Muckova, M. Schmidt, D. Herman, A. Dlabkova, J. Pejchal, D. Jun, Simultaneous determination of malondialdehyde and 3-nitrotyrosine in cultured human hepatoma cells by liquid chromatography–mass spectrometry, Biomed. Chromatogr. 32 (12) (2018) e4349.
[15] M. Kaykhaii, H. Yahyavi, M. Hashemi, M.R. Khoshroo, A simple graphene-based pipette tip solid-phase extraction of malondialdehyde from human plasma and its determination by spectrofluorometry, Anal. Bioanal. Chem. 408 (18) (2016) 4907–4915.
[16] A. Fashi, M. Cheraghi, H. Ebadipur, H. Ebadipur, A. Zamani, H. Badiee, S. Pedersen-Bjergaard, Exploiting agarose gel modified with glucose-fructose syrup as a green sorbent in rotating-disk sorptive extraction technique for the determination of trace malondialdehyde in biological and food samples, Talanta 217 (2020), 121001.
[17] R. Liu, A. Simple, Low-Cost and Efficient β-CD/MWCNTs/CP-based Electrochemical Sensor for the Rapid and Sensitive Detection of Methyl Parathion, Int. J. Electrochem. Sci. (2019) 9785–9795.
[18] S.I. Kaya, A. Cetinkaya, N.K. Bakirhan, S.A. Ozkan, Trends in sensitive electrochemical sensors for endocrine disruptive compounds, Trends Environ. Anal. Chem. 28 (2020) e00106.
[19] M. Hasanzadeh, F. Mokhtari, V. Jouyban-Gharamaleki, A. Mokhtarzadeh, N. Shadjou, Electrochemical monitoring of malondialdehyde biomarker in biological samples via electropolymerized amino acid/chitosan nanocomposite, J. Mol. Recognit. 31 (8) (2018) e2717.
[20] M. Hasanzadeh, F. Mokhtari, N. Shadjou, A. Eftekhari, A. Mokhtarzadeh, V. Jouyban-Gharamaleki, S. Mahboob, Poly arginine-graphene quantum dots as a biocompatible and non-toxic nanocomposite: Layer-by-layer electrochemical preparation, characterization and non-invasive malondialdehyde sensory application in exhaled breath condensate, Mater. Sci. Eng., C 75 (2017) 247–258.
[21] M. Zamani-Kalajahi, M. Hasanzadeh, N. Shadjou, M. Khoubnasabjafari, K. Ansarin, V. Jouyban-Gharamaleki, A. Jouyban, Electrodeposition of taurine on gold surface and electro-oxidation of malondialdehyde, Surfae, Engineering. 31 (3) (2015) 194–201.
[22] L. Yuan, Y. Lan, M. Han, J. Bao, W. Tu, Z. Dai, Label-free and facile electrochemical biosensing using carbon nanotubes for malondialdehyde detection, Analyst. 138 (2013) 3131–3134.
[23] D. Işık, S. Şahin, M.O. Caglayan, Z. Üstündağ, Electrochemical impedimetric detection of kanamycin using molecular imprinting for food safety, Microchem. J. 160 (2021), 105713.
[24] C. Su, Z. Li, D. Zhang, Z. Wang, X. Zhou, L. Liao, X. Xiao, A highly sensitive sensor based on a computer-designed magnetic molecularly imprinted membrane for the determination of acetaminophen, Biosens. Bioelectron. 148 (2020), 111819.
[25] B.B. Prasad, R. Singh, A. Kumar, Synthesis of fullerene (C60-monoadduct)-based water-compatible imprinted micelles for electrochemical determination of chlorambucil, Biosens. Bioelectron. 94 (2017) 115–123.
[26] R. Xing, S. Wang, Z. Bie, H. He, Z. Liu, Preparation of molecularly imprinted polymers specific to glycoproteins, glycans and monosaccharides via boronate affinity controllable–oriented surface imprinting, Nat. Protoc. 12 (5) (2017) 964–987.
[27] T.A. do Nascimento, H.L. de Oliveira, K.B. Borges, Magnetic molecularly imprinted polypyrrole as a new selective adsorbent for pharmaceutically active compounds, Journal of Environmental Chemical Engineering. 7 (2019) 103371.
[28] M.-H. Lee, K.-T. Liu, J.L. Thomas, Z.-L. Su, D. O'Hare, T. van Wuellen, J. M. Chamarro, S. Bolognin, S.-C. Luo, J.C. Schwamborn, H.-Y. Lin, Peptide-Imprinted Poly(hydroxymethyl 3,4-ethylenedioxythiophene) Nanotubes for Detection of α Synuclein in Human Brain Organoids, ACS Applied Nano Materials. 3 (8) (2020) 8027–8036.
[29] L. Xu, J. Li, J. Zhang, J. Sun, T. Gan, Y. Liu, A disposable molecularly imprinted electrochemical sensor for the ultra-trace detection of the organophosphorus insecticide phosalone employing monodisperse Pt-doped UiO-66 for signal amplification, Analyst. 145 (9) (2020) 3245–3256.
[30] Y. Zhu, Y. Feng, S. Chen, M. Ding, J. Yao, Carbon nitride nanotube-based materials for energy and environmental applications: a review of recent progresses, J. Mater. Chem. A 8 (2020) 25626–25648.
[31] S. Torres-Cartas, M. Catalá-Icardo, S. Meseguer-Lloret, E.F. Simó-Alfonso, J. M. Herrero-Martínez, Recent advances in molecularly imprinted membranes for sample treatment and separation, Separations. 7 (2020) 1–28.
[32] M. Amatatongchai, W. Sroysee, P. Sodkrathok, N. Kesangam, S. Chairam, P. Jarujamrus, Novel three-Dimensional molecularly imprinted polymer-coated carbon nanotubes (3D-CNTs@MIP) for selective detection of profenofos in food, Anal. Chim. Acta 1076 (2019) 64–72.
[33] M. Dehghani, N. Nasirizadeh, M.E. Yazdanshenas, Determination of cefixime using a novel electrochemical sensor produced with gold nanowires/graphene oxide/electropolymerized molecular imprinted polymer, Mater. Sci. Eng., C 96 (2019) 654–660.
[34] D. Duan, H. Yang, Y. Ding, L. Li, G. Ma, A three-dimensional conductive molecularly imprinted electrochemical sensor based on MOF derived porous carbon/carbon nanotubes composites and prussian blue nanocubes mediated amplification for chiral analysis of cysteine enantiomers, Electrochim. Acta 302 (2019) 137–144.
[35] D. Wang, J. Wang, J. Zhang, Y. Li, Y. Zhang, Y. Li, B.C. Ye, Novel electrochemical sensing platform based on integration of molecularly imprinted polymer with Au@Ag hollow nanoshell for determination of resveratrol, Talanta 196 (2019) 479–485.
[36] M. Afzali, A. Mostafavi, T. Shamspur, A novel electrochemical sensor based on magnetic core@shell molecularly imprinted nanocomposite (Fe3O4@graphene oxide@MIP) for sensitive and selective determination of anticancer drug capecitabine, Arabian J. Chem. 13 (8) (2020) 6626–6638.
[37] R.R. Zhang, J. Zhan, J.J. Xu, J.Y. Chai, Z.M. Zhang, A.L. Sun, J. Chen, X.Z. Shi, Application of a novel electrochemiluminescence sensor based on magnetic glassy carbon electrode modified with molecularly imprinted polymers for sensitive monitoring of bisphenol A in seawater and fish samples, Sens. Actuators, B 317 (2020), 128237.
[38] P. Montoro-Leal, J.C. García-Mesa, M. del M. López Guerrero, E. Vereda Alonso, Comparative Study of Synthesis Methods to Prepare New Functionalized Adsorbent Materials Based on MNPs–GO Coupling, Nanomaterials. 10 (2020) 304.
[39] S.Y. Zhao, D.-G. Lee, C.-W. Kim, H.-G. Cha, Y.-H. Kim, Y.-S. Kang, Synthesis of Magnetic Nanoparticles of Fe3O4 and CoFe2O4 and Their Surface Modification by Surfactant Adsorption, Bull. Korean Chem. Soc. 27 (2006) 237–242.
[40] W.S. Hummers, R.E. Offeman, Preparation of Graphitic Oxide, Journal of the American Chemical Society. 80 (1958) 1339–1339.
[41] J.-P. Steghens, A.L. van Kappel, I. Denis, C. Collombel, Diaminonaphtalene, a new highly specific regent for HPLC-UV measurement of total and free malondialdehyde in human plasma or serum, Free Radical Biol. Med. 31 (2) (2001) 242–249.
[42] J. Yang, X. Zhang, Y. Mijiti, Y. Sun, M. Jia, Z. Liu, Y. Huang, H.A. Aisa, Improving performance of molecularly imprinted polymers prepared with template of low purity utilizing the strategy of macromolecular crowding, J. Chromatogr. A 1624 (2020), 461155.
[43] G. Wang, Optical and electrochemical investigation of diaminonaphthalene derivatives, Synth. Met. 160 (7-8) (2010) 599–603.
[44] X. Wang, X. Liu, T. Cheng, H. Li, X.F. Yang, Development of 4-hydrazinyl-7-nitrobenzofurazan as a fluorogenic probe for detecting malondialdehyde in biological samples, Sensors and Actuators, B, Chemical. 254 (2018) 248–254.
[45] A. Safavi, R. Ahmadi, A.M. Ramezani, Vortex-assisted liquid-liquid microextraction based on hydrophobic deep eutectic solvent for determination of malondialdehyde and formaldehyde by HPLC-UV approach, Microchem. J. 143 (2018) 166–174.
[46] R. Malaei, A.M. Ramezani, G. Absalan, Analysis of malondialdehyde in human plasma samples through derivatization with 2,4-dinitrophenylhydrazine by ultrasound-assisted dispersive liquid–liquid microextraction-GC-FID approach, J. Chromatogr., B: Anal. Technol. Biomed. Life Sci. 1089 (2018) 60–69.